The phase-only null beamforming synthesis via manifold optimization

Yang Cong[1,2],Jinfeng Hu*[1,2], Kai Zhong[1,2], Jie Wu[1,2]

[1]Yangtze Delta Region Institute (Quzhou), University of Electronic Science and Technology of China
Quzhou, Zhejiang,324000
[2]the school of Information and Communication Engineering, University of Electronic Science and Technology of China
Chengdu, 611731
* Email: hujf@uestc.edu.cn

IGARSS 2022 - 2022 IEEE International Geoscience and Remote Sensing Symposium | 978-1-6654-2792-0/22/$31.00 ©2022 IEEE | DOI: 10.1109/IGARSS46834.2022.9883605

***Abstract*—The phase-only beamforming synthesis is widely applied in millimeter wave communication, radar and sonar. Due to the CMC, the problem is non-convex. The most current methods solve the problem by designing the phase, which either degrades the performance or needs huge complexity. To address this issue, a low-complexity Riemannian Manifold Optimization based Conjugate Gradient (RMOCG) method is proposed. First, the original problem is transformed into an unconstrained problem on a complex circle manifold. Then, a RMOCG algorithm is derived, by deriving the gradient descent direction and the step size for ensuring the cost function non-increasing. Comparing with the existing methods, the proposed method has the following advantages: 1) the null depth is respectively 8 dB deeper than [6] and 3 dB deeper than [12]. 2) The computational cost is 2 magnitude lower than [6] and 1 magnitude lower than [12].**

***Index Terms*—phase-only beamforming, constant modulus, Riemannian manifold, RMOCG method**

I. Introduction

The beamforming synthesis with the constant modulus constraint(CMC) is the key issue in the fields of radar and communication. The interference can be suppressed with the null beaforming, which can enhance the Signal to Interference plus Noise Ratio(SINR)[1, 2]. Moreover, the beamforming with CMC is more practical in engineering application. Therefore, the beamforming synthesis with CMC has received extensive attention [3–12].

Due to the CMC, the beamforming problem is non-convex [13]. At present, the existing methods are mainly divided into two categories. In the first category, the beamforming is designed by relaxing the CMC [4, 5]. The second category is designing phase.

In the above methods, the designing phase method attracts extensive attention [7–12]. In [7], A typical gradient projection is proposed by converting the problem into the unconstrained phase design problem. Nevertheless, the convergence may become slow, due to the choose of the stepsize. To address this issue, an Alternating Direction Method Of Multipliers(ADMM) method is proposed in [8], by dividing the problem into multiple blocked problems. Nevertheless, the convergence is sensitive to the initial parameters. To address the issue, a Deep Learning based method is proposed in [10, 11] by designing the phase optimization network. However, huge computational cost is needed due to the complex neural network. To reduce the complexity, a convex relaxation(CR) method is proposed in [6, 14], by relaxing the problem into convex phase optimization problem. Nevertheless, the performance degrades due to the relaxation. To enhance the performance,a dual-phase-shifter (DPS) method is proposed in [12], by designing double phases.Nevertheless, the complexity is not reduced very much due to the dual phase shifters structure.

To address the issues above, a low-complexity Riemannian Manifold Optimization based Conjugate Gradient (RMOCG) method is proposed. First, the original problem is transformed into an unconstrained problem on a complex circle manifold. Then, a RMOCG algorithm is derived, by deriving the gradient descent direction and the step size for ensuring the cost function non-increasing. The main contributions are concluded as follows.

- The null depth is respectively 8 dB deeper than [6] and 3 dB deeper than [12].
- The computational cost is 2 magnitude lower than [6] and 1 magnitude lower than [12], respectively.

II. System Model and Problem Formulation

We consider an one-dimensional M-element antenna array. The steering vector of the linear antenna array is

$$\boldsymbol{a}(\theta) = [1, e^{j2\pi r_2 \sin\theta/\lambda}, \cdots, e^{j2\pi r_M \sin\theta/\lambda}]^T, \quad (1)$$

where r_m,$m = 1, 2, \cdots M$ is the distance from the m-th array element to the reference array element, $\theta \in \Theta = [-\frac{\pi}{2}, \frac{\pi}{2}]$ is the direction of arrival (DOA), λ is the wavelength and $(\cdot)^T$ is the transpose operation.

Then the energy in the direction of θ is denoted as

$$G(\theta) = |\boldsymbol{w}^H \boldsymbol{a}(\theta)|^2 = \boldsymbol{w}^H \boldsymbol{a}(\theta)\boldsymbol{a}(\theta)^H \boldsymbol{w} = \boldsymbol{w}^H \mathbf{X}(\theta)\boldsymbol{w}, \quad (2)$$

where $\mathbf{X}(\theta) = \boldsymbol{a}(\theta)\boldsymbol{a}(\theta)^H \in \mathbb{C}^{M\times M}$, $\boldsymbol{w} = [w(1), w(2), \cdots w(M)]^T \in \mathbb{C}^{M\times 1}$ is the weighted vector.

Interference is always accompanied by signal transmission. When the signal gain in the main lobe direction meets the requirements we need, we turn to consider suppressing the interference in the side lobe direction. The problem can be formulated as

$$\begin{array}{ll} \min\limits_{\boldsymbol{w}} & \boldsymbol{w}^H\mathbf{Y}(\theta_i)\boldsymbol{w} \\ s.t. & \begin{array}{l}\boldsymbol{w}^H\mathbf{X}(\theta_0)\boldsymbol{w} \geq A_0 \\ |w(m)| = 1, m = 1, 2, \cdots M\end{array} \end{array}, \tag{3}$$

where $\mathbf{Y}(\theta_i) = \sum\limits_{\theta_i \in \Theta_i} \mathbf{X}(\theta_i)$, θ_i is the undesired direction, Θ_i is the set of the total undesired directions, θ_0 is the desired direction, A_0 is the signal gain requirement of the main lobe direction, and $|w(m)| = 1$ is the CMC.

III. The Proposed Method

In this section, a low-complexity RMOCG method is proposed. First, the original problem is transformed into an unconstrained problem on a complex circle manifold. Then,a RMOCG algorithm is derived, by deriving the gradient descent direction and the step size.

A. Problem Transformation

The problem in (3) can be geometrically transformed into an unconstrained problem on a complex circle manifold as

$$\left\{ \begin{array}{ll} \min\limits_{\boldsymbol{w}\in\Omega} & \boldsymbol{w}^H\mathbf{Y}(\theta_i)\boldsymbol{w} \\ s.t. & \boldsymbol{w}^H\mathbf{X}(\theta)\boldsymbol{w} \geq A_0 \end{array} \right. , \tag{4}$$

where

$$\Omega = \left\{ w \in C^M \big| |w(m)| = 1, m = 1, 2, \cdots M \right\}, \tag{5}$$

where Ω is the complex circle manifold.

Using the Lagrangian multiplier method, the problem in (4) can be written as

$$\min\limits_{\boldsymbol{w}\in\Omega} \quad \boldsymbol{w}^H\mathbf{Y}(\theta_i)\boldsymbol{w} + \rho\left(A_0 - \boldsymbol{w}^H\mathbf{X}(\theta)\boldsymbol{w}\right), \tag{6}$$

where $\rho > 0$ is the Lagrange multiplier.

The problem in (6) can be simplified as

$$\min\limits_{\boldsymbol{w}\in\Omega} \quad f(\boldsymbol{w}) = \boldsymbol{w}^H\mathbf{P}\boldsymbol{w}, \tag{7}$$

where $\mathbf{P} = \mathbf{Y}(\theta_i) + \rho(\frac{A_0}{M}\mathbf{I}_M - \mathbf{X}(\theta))$.

The problem in (7) is an unconstrained optimisation problem on the manifold. It can be solved by the gradient descent approaches.

B. The Proposed RMOCG Algorithm

In this section, a RMOCG algorithm is proposed. First, calculate the Riemann gradient; Second, derive the descent direction; third, find the step size with the Armijo line search strategy; and finally, iteratively update the feasible solution until convergence.

1) Obtain the Riemann gradient: The Riemann gradient is obtained by projecting the Euclidean gradient onto the tangent space. In the i-th iteration, it is denoted as

$$\begin{aligned} &\nabla_\Omega f(\boldsymbol{w}_i) = P_{T_{\boldsymbol{w}_i}\Omega}(\nabla f(\boldsymbol{w}_i)) \\ &= \nabla f(\boldsymbol{w}_i) - \Re(\nabla f(\boldsymbol{w}_i) \odot {\boldsymbol{w}_i}^*) \odot {\boldsymbol{w}_i}^T \end{aligned}, \tag{8}$$

where

- $T_{\boldsymbol{w}_i}\Omega$ is a tangent space consisting of all tangent vectors at points in the point space Ω. It can be given as
$$T_{\boldsymbol{w}_i}\Omega = \left\{ \boldsymbol{s} \in C^M | \Re(\boldsymbol{s} \odot {\boldsymbol{w}_i}^*) = 0_M \right\}, \tag{9}$$
where $\Re(\cdot)$ is the operator to obtain the real part, $\odot$ is the Hadamard product operator.
- $P_{T_{\boldsymbol{w}_i}\Omega}$ is a projection operator from the Riemannian space to the tangent space, which is given as
$$P_{T_{\boldsymbol{w}_i}\Omega}(\boldsymbol{x}) = \boldsymbol{x} - \Re(\boldsymbol{x} \odot {\boldsymbol{w}_i}^*) \odot {\boldsymbol{w}_i}^T, \tag{10}$$
where $\boldsymbol{x}$ is an arbitrary vector.
- $\nabla f(w_i)$ is the Euclidean gradient, which is
$$\nabla f(\boldsymbol{w}_i) = 2\mathbf{P}\boldsymbol{w}_i. \tag{11}$$

2) Derive the descent direction: The Polak-Ribiere conjugate gradient descent direction, ensuring the algorithm to converge superlinearly, is used to compute the descent direction. In the i-th iteration, the descent direction is

$$\boldsymbol{d}_i = -\nabla_\Omega f(\boldsymbol{w}_i) + {\beta_i}^{PR} T_{\boldsymbol{w}_{i-1}\to\boldsymbol{w}_i}\Omega(\boldsymbol{d}_{i-1}), \tag{12}$$

where $T_{\boldsymbol{w}_{i-1}\to\boldsymbol{w}_i}\Omega(\bullet)$ is the vector transfer operation required to add and subtract points on different tangent spaces, which is denoted as

$$T_{\boldsymbol{w}_{i-1}\to\boldsymbol{w}_i}\Omega(\boldsymbol{d}_{i-1}) = \boldsymbol{d}_{i-1} - \Re(\boldsymbol{d}_{i-1} \odot {\boldsymbol{w}_i}^*) \odot \boldsymbol{w}_i, \tag{13}$$

${\beta_i}^{PR}$ is the Polak-Ribieres conjugate parameter,which is

$${\beta_i}^{PR} = [\nabla_\Omega f(\boldsymbol{w}_i)]^H \frac{\nabla_\Omega f(\boldsymbol{w}_i) - T_{\boldsymbol{w}_{i-1}\to\boldsymbol{w}_i}\Omega(\nabla_\Omega f(\boldsymbol{w}_i))}{||\nabla_\Omega f(\boldsymbol{w}_{i-1})||^2}. \tag{14}$$

3) Derive the step size: The step size is found based on the well-known Armijo line search strategy, which guarantees the objective function not increasing. The essence is to find the smallest integer h satisfying

$$f(\boldsymbol{w}_i) - f(\boldsymbol{w}_i + \tau_{i-1}\beta^h\boldsymbol{d}_i) \geq \sigma\tau_{i-1}\beta^h||\nabla_\Omega f(\boldsymbol{w}_i)||^2, \tag{15}$$

where $h > 0$, $\sigma, \beta \in (0, 1), \tau_{i-1} > 0$.

Therefore, the step size of the i-th iteration is denoted as

$$\tau_i = \tau_{i-1}\beta^h. \tag{16}$$

4) Update the feasible solution: The solution on the tangent space is denoted as

$$\bar{\boldsymbol{w}}_i = \boldsymbol{w}_i + \tau_i\boldsymbol{d}_i. \tag{17}$$

The feasible solution at the $i+1$-th iteration is obtained by retracting the solution in (17) back onto the complex circle manifold, which is given as

$$\boldsymbol{w}_{i+1} = \bar{\boldsymbol{w}}_i \oslash |\bar{\boldsymbol{w}}_i| \tag{18}$$

where $\oslash$ is the Hadamard element-wise deviation operator, $|\bar{\boldsymbol{w}}_i|$ the modulus of this element.

Based on the above discussions, the proposed method is summarized as **Algorithm 1**.

Algorithm 1 :The RMOCG algorithm for solving (7)

Input: $I = 1500, \varepsilon = 10^{-3}$

Output: $\boldsymbol{w}^* = \boldsymbol{w}_{i+1}$

1: Set initial value, initial descent direction, initial stepsize $\boldsymbol{w}_0 \in \Omega, \boldsymbol{d}_0 = -\nabla_\Omega f(\boldsymbol{w}_0), \tau_0 = 10$;

2: $\boldsymbol{w}_1 = (\boldsymbol{w}_0 + \tau_0 \boldsymbol{d}_0) \oslash |\boldsymbol{w}_0 + \tau_0 \boldsymbol{d}_0|$

While $||\nabla_\Omega f(\boldsymbol{w}_{i-1})|| \geq \varepsilon$ and $i \leq I$ do

3: Calculate the Riemann gradient.
Use equation (11) to calculate $\nabla f(\boldsymbol{w}_i)$
Calculate $\nabla_\Omega f(\boldsymbol{w}_i)$ using equation (8)

4: Compute the direction of descent
Calculate $T_{\boldsymbol{w}_{i-1} \to \boldsymbol{w}_i} \Omega(\boldsymbol{d}_{i-1})$ using formula(13)
Calculate β_i^{PR} with formula(14)
Calculate $\boldsymbol{d}_i$ using formula (12)

5: Calculate step size τ_i using formula (16)

6: Update calculation iterations
Calculate $\bar{\boldsymbol{w}}_i$ with formula (17)
Calculate $\boldsymbol{w}_{i+1}$ with formula (18)

7: Loop calculation $i = i + 1$

C. *Complexity Analysis*

The complexity of each iteration is analysed as follows.

TABLE I: Complexity Analysis

The iteration procedures	Calculation complexity
Riemannian gradient	$M^2 + 2M$ multiplications
Descent direction	$(5M)$ and M divisions.
Step size	$(h+1)M^2 + (h+1)M$ multiplications.
Update solution	M multiplications and M divisions.
Each iteration	$((h+2)M^2 + (h+11)M)$

As shown in TABLE I, the complexity of the proposed method is $O(M^2)$, while the complexity of the method in [6, 12] is $O(M^3)$

IV. Numerical results

In this section, several simulations are shown to evaluate the performance of the convergence, nulling depth and computational time. For comparison purpose, the convex relaxation (CR) method in [6] and the dual phase shifter (DPS) method in [12] are considered.

The simulation configuration is set as follows. *Case* I:The number of antennas is $M = 64$, the target direction is $\theta_0 = 10°$, and the interference direction is $\theta_i = \{-49° : -40°\}$. *Case* II: The number of antennas is $M = 64$, the target direction is $\theta_0 = -30°$, and the interference direction is $\theta_i = \{10° : 20°\}$.

A. *The convergence evaluation*

Fig.1 shows the cost function versus the number of iterations in *Case* I and Case II. As can be seen, the fast convergence is obtained.

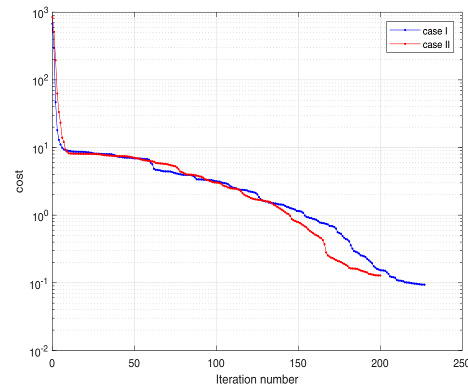

Fig. 1: The cost function versus the number of the iterations.

B. *The nulling beamforming comparison*

Fig.2 shows the nulling beamforming in *Case* I. As shown in Fig.2, the null of the proposed method are respectively 8dB deeper than [6] and 3dB deeper than [12].

Fig.3 shows the nulling beamforming in *Case* II. As shown in Fig.3, the average null of the proposed method is respectively 5 dB deeper than [6] and 0.5 dB deeper than [12].

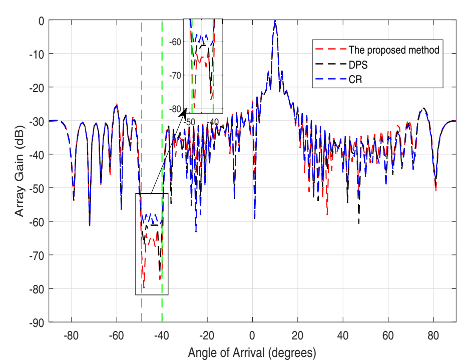

Fig. 2: The formed beam pattern in case I.

C. *The computational cost camparison*

Fig.4 shows the computational cost versus the number of antennas. As can be seen, the computational cost is 2 magnitude lower than [6] and 1 magnitude lower than [12], respectively. Moreover, as the number of the antennas increasing, more obvious priority is shown in the proposed method.

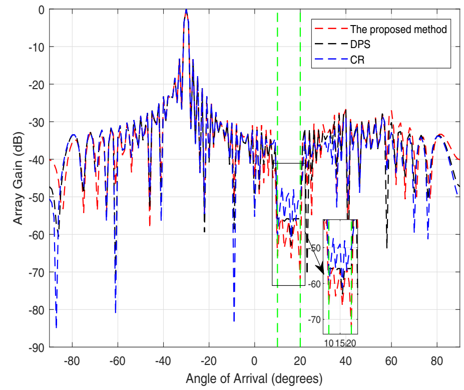

Fig. 3: The formed beam pattern in case II.

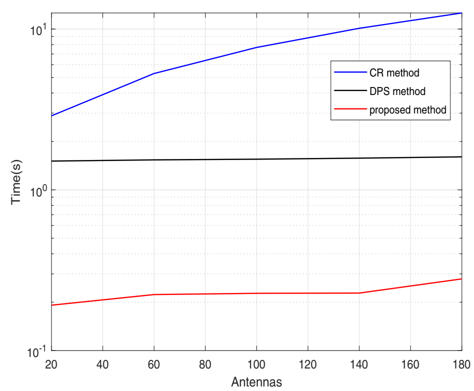

Fig. 4: Computational time versus number of antennas.

V. Conclusion

In this paper, a low-complexity Riemannian Manifold Optimization based Conjugate Gradient (RMOCG) method is proposed for phase only null beamforming synthesis. First, the original problem is transformed into an unconstrained problem on a complex circle manifold. Then, a RMOCG algorithm is derived, by deriving the gradient descent direction and the step size for ensuring the cost function non-increasing. Comparing with the existing methods, the proposed method has better performance in terms of the null depth and the computational cost.

VI. Acknowledgment

This work was supported by the National Natural Science Foundation of China under Grant 61871102 and 61731006.This work was also supported by the Municipal Government of Quzhou under Grant Number 2021D001.

References

[1] A. Khzmalyan and A. Kondratiev, "The phase-only shaping and adaptive nulling of an amplitude pattern," *IEEE Transactions on Antennas and Propagation*, vol. 51, no. 2, pp. 264–272, 2003.

[2] G. Buttazzoni and R. Vescovo, "Power synthesis for reconfigurable arrays by phase-only control with simultaneous dynamic range ratio and near-field reduction," *IEEE Transactions on Antennas and Propagation*, vol. 60, no. 2, pp. 1161–1165, 2012.

[3] B. Fuchs, "Application of convex relaxation to array synthesis problems," *IEEE Transactions on Antennas and Propagation*, vol. 62, no. 2, pp. 634–640, 2014.

[4] Y. Liu, J. Bai, K. D. Xu, Z. Xu, F. Han, Q. H. Liu, and Y. Jay Guo, "Linearly polarized shaped power pattern synthesis with sidelobe and cross-polarization control by using semidefinite relaxation," *IEEE Transactions on Antennas and Propagation*, vol. 66, no. 6, pp. 3207–3212, 2018.

[5] X. Zhang, Z. He, X. Zhang, and W. Peng, "High-performance beampattern synthesis via linear fractional semidefinite relaxation and quasi-convex optimization," *IEEE Transactions on Antennas and Propagation*, vol. 66, no. 7, pp. 3421–3431, 2018.

[6] P. Cao, J. S. Thompson, and H. Haas, "Constant modulus shaped beam synthesis via convex relaxation," *IEEE Antennas and Wireless Propagation Letters*, vol. 16, pp. 617–620, 2017.

[7] M. Zhang, J. Li, S. Zhu, and X. Chen, "Fast and simple gradient projection algorithms for phase-only beamforming," *IEEE Transactions on Vehicular Technology*, vol. 70, no. 10, pp. 10620–10632, 2021.

[8] C. G. Tsinos and B. Ottersten, "An efficient algorithm for unit-modulus quadratic programs with application in beamforming for wireless sensor networks," *IEEE Signal Processing Letters*, vol. 25, no. 2, pp. 169–173, 2018.

[9] C. G. Tsinos, A. A. Rontogiannis, and K. Berberidis, "Distributed blind hyperspectral unmixing via joint sparsity and low-rank constrained non-negative matrix factorization," *IEEE Transactions on Computational Imaging*, vol. 3, no. 2, pp. 160–174, 2017.

[10] M. A. Almagboul, F. Shu, and A. M. S. Abdelgader, "Deep-learning-based phase-only robust massive mu-mimo hybrid beamforming," *IEEE Communications Letters*, vol. 25, no. 7, pp. 2280–2284, 2021.

[11] T. Lin and Y. Zhu, "Beamforming design for large-scale antenna arrays using deep learning," *IEEE Wireless Communications Letters*, vol. 9, no. 1, pp. 103–107, 2020.

[12] Y. Zhuang, X. Zhang, and Z. He, "Beampattern synthesis for phased array with dual-phase-shifter structure," *IEEE Transactions on Antennas and Propagation*, vol. 69, no. 10, pp. 7053–7058, 2021.

[13] S. Sojoudi and J. Lavaei, "On the exactness of semidefinite relaxation for nonlinear optimization over graphs: Part i," in *52nd IEEE Conference on Decision and Control*, pp. 1043–1050, 2013.

[14] Q. Lu, G. Cui, R. Liu, and X. Yu, "Beampattern synthesis via first-order iterative convex approximation," *IEEE Antennas and Wireless Propagation Letters*, vol. 20, no. 8, pp. 1493–1497, 2021.